PHILOSOPHICAL TRANSACTIONS B

rstb.royalsocietypublishing.org

Research

Cite this article: Fontes CG *et al*. 2018 Dry and hot: the hydraulic consequences of a climate change–type drought for Amazonian trees. *Phil. Trans. R. Soc. B* **373**: 20180209. http://dx.doi.org/10.1098/rstb.2018.0209

Accepted: 17 August 2018

One contribution of 22 to a discussion meeting issue 'The impact of the 2015/2016 El Niño on the terrestrial tropical carbon cycle: patterns, mechanisms and implications'.

Subject Areas:
ecology, environmental science, plant science

Keywords:
Amazon rainforest, drought, leaf and xylem safety margins, turgor loss point, xylem embolism, 2015–2016 El Niño

Author for correspondence:
Clarissa G. Fontes
e-mail: clafontes@berkeley.edu

Electronic supplementary material is available online at https://dx.doi.org/10.6084/m9.figshare.c.4213235.

THE ROYAL SOCIETY PUBLISHING

Dry and hot: the hydraulic consequences of a climate change–type drought for Amazonian trees

Clarissa G. Fontes[1], Todd E. Dawson[1,2], Kolby Jardine[3,4], Nate McDowell[5], Bruno O. Gimenez[4], Leander Anderegg[1], Robinson Negrón-Juárez[3], Niro Higuchi[4], Paul V. A. Fine[1], Alessandro C. Araújo[6,7] and Jeffrey Q. Chambers[3,8]

[1]Department of Integrative Biology, University of California at Berkeley, Berkeley, CA 94720, USA
[2]Ecosystem Science Division, Department of Science, Policy and Management, Environmental University of California Berkeley, Berkeley, CA, USA
[3]Climate Science Department, Climate and Ecosystem Sciences Division, Lawrence Berkeley National Laboratory, One Cyclotron Road, Building 74, Berkeley, CA 94720, USA
[4]Ciências de Florestas Tropicais, Instituto Nacional de Pesquisas da Amazônia (INPA), Manaus-AM 69067-375, Brazil
[5]Pacific Northwest National Laboratory, Richland, WA, USA
[6]Department of Global Ecology, Carnegie Institution for Science, 260 Panama St., Stanford, CA 94305, USA
[7]Embrapa Amazônia Oriental, Trav. Dr. Enéas Pinheiro, Belém, Pará 66095-100, Brazil
[8]Department of Geography, University of California Berkeley, 507 McCone Hall #4740, Berkeley, CA 94720, USA

CGF, 0000-0003-4712-3764; KJ, 0000-0001-8491-9310; BOG, 0000-0001-7336-9448; LA, 0000-0002-5144-7254; RN-J, 0000-0002-4691-2692

How plants respond physiologically to leaf warming and low water availability may determine how they will perform under future climate change. In 2015–2016, an unprecedented drought occurred across Amazonia with record-breaking high temperatures and low soil moisture, offering a unique opportunity to evaluate the performances of Amazonian trees to a severe climatic event. We quantified the responses of leaf water potential, sap velocity, whole-tree hydraulic conductance (K_{wt}), turgor loss and xylem embolism, during and after the 2015–2016 El Niño for five canopy-tree species. Leaf/xylem safety margins (SMs), sap velocity and K_{wt} showed a sharp drop during warm periods. SMs were negatively correlated with vapour pressure deficit, but had no significant relationship with soil water storage. Based on our calculations of canopy stomatal and xylem resistances, the decrease in sap velocity and K_{wt} was due to a combination of xylem cavitation and stomatal closure. Our results suggest that warm droughts greatly amplify the degree of trees' physiological stress and can lead to mortality. Given the extreme nature of the 2015–2016 El Niño and that temperatures are predicted to increase, this work can serve as a case study of the possible impact climate warming can have on tropical trees.

This article is part of a discussion meeting issue 'The impact of the 2015/2016 El Niño on the terrestrial tropical carbon cycle: patterns, mechanisms and implications'.

1. Introduction

The palaeoecological records show that the Amazon Basin has experienced droughts in the past [1–3]; however, the frequency, duration and intensity of these climatic events have recently accelerated, imposing a novel and significant challenge for plant communities [4–6]. Currently, there is a lack of *in situ* data on how the combination of high leaf temperature and low soil water may impact the way plants regulate their water consumption in the tropics. In 2015–2016, a strong El Niño occurred, with record-breaking high temperatures and low precipitation [7], offering a unique opportunity to evaluate how Amazonian trees in their natural environment respond physiologically to severe changes in water supply and demand.

Future droughts are projected to become increasingly severe due to warming [8]. Air warming intensifies tree stress by driving a nonlinear increase in vapour pressure deficit (VPD), causing greater water loss through plant stomata and from the soil surface [9–11]. Moreover, canopy leaves in tropical forests are usually warmer than air temperature, and an increase of 3°C in air temperature can elevate VPD by 45% [12]. Studies show that leaf photosynthesis and stomatal conductance decline at leaf temperatures above the optimal value of around 30–35°C [5,13], and trees are also at a greater risk of losing water transport capacity or suffering hydraulic failure during hot droughts [14–16]. Because wet tropical ecosystems are thermally stable, many tropical plants may lack the ability to avoid highly negative xylem pressure caused by extreme climate warming [13,17,18].

Plant hydraulic characteristics are thought to play a critical role in survival during drought (e.g. [19–21]). Traits commonly used as indicators of plant water stress tolerance are the leaf water potential at the turgor loss point (Ψ_{tlp}) and stem xylem vulnerability to cavitation [22–24]. These two traits represent live (leaf cells) and dead (xylem) tissues that play key roles in plant performance and survival. Oddly, few studies on tropical trees have measured both of these traits and therefore may give us an incomplete picture of a plant's resistance, tolerance and overall response to high temperature and water deficit.

Leaf turgor loss (π_{tlp}) or leaf wilting point is a useful metric to quantify leaf and plant drought tolerance and is usually calculated using leaf pressure–volume (PV) curves [22,25]. A more negative π_{tlp} enables a plant to acquire water from drier soils and to maintain leaf function at lower leaf water potentials [19,22]. Similarly, plants' ability to resist xylem cavitation at high xylem tension is advantageous because it allows them to transport water and fix CO_2 under drier conditions [24]. The most commonly used indexes of xylem embolism resistance are Ψ_{50} and Ψ_{88}, quantified as the value of xylem water potential (Ψ_x) causing 50 or 88% loss of xylem hydraulic conductivity (e.g. [20,26,27]). These leaf and xylem metrics (π_{tlp}, Ψ_{50} and Ψ_{88}) can then be used to calculate hydraulic safety margins (SMs) [28].

Here, we present 2 years of leaf and xylem physiological measurements, along with climatic data to investigate how the combination of high atmospheric water demand and low water supply, imposed by the 2015–2016 El Niño, impacted the performance of five different Amazonian tree species. We present local climatic and environmental data to characterize the soil water deficit (supply) and the increase in VPD (demand) during the 2015–2016 drought. Then, we test the following hypotheses: (i) species' leaf and xylem hydraulic SMs will narrow with an increase in VPD or decrease in soil water supply; (ii) the decline in sap velocity during the drought will be mainly explained by a decrease in whole-tree hydraulic conductance caused by increased xylem resistance due to a spread in xylem embolism.

2. Material and methods

(a) Study site

The study was conducted at the 55 m K34 tower (2°35.37′S, 60°06.92′W), situated 3 km away from the main dirt road in the Reserva Biológica do Cueiras and located 90 km north-northwest of the city of Manaus, Brazil [29]. The site (known as ZF-2) is administered by INPA (Instituto Nacional de Pesquisas da Amazônia) under the Large-scale Biosphere–Atmosphere Experiment in Amazonia (LBA) programme. The mean monthly temperature is 26°C, and annual rainfall is around 2000–2600 mm, with a dry season between July and September [30,31]. The vegetation in this area is old-growth, *terra-firme* rainforest, with a leaf area index of 5–6 and an average canopy height of 30 m. The soil on this medium-size plateau area is mainly Oxisols with high clay content [32].

(b) Plant measurements and experimental protocols

Leaf water potential, sap velocity and PV measurements were sampled from five tree species (one individual per species) around K34 tower. *Pouteria anomala* ((Pires) T.D.Penn.) (Sapotaceae) 35.3 cm in diameter at breast height (DBH, 1.3 m) and 31 m in height, *Pouteria erythrochrysa* (T.D.Penn) (Sapotaceae) with 36.5 cm of DBH and 29.3 m in height, *Eschweilera cyathiformis* (S.A.Mori) (Lecythidaceae) with 14.3 cm of DBH and 19.8 m in height, *Couepia longipendula* (Pilg.) (Chrysobalanaceae) with 28.1 cm of DBH and 23.9 m in height and *Eschweilera* sp. (Mart. ex DC.) with 29.7 cm of DBH and 27.8 m in height. These three genera encompass approximately 25% of all individuals found in the area (based on unpublished studies in permanent plots located approx. 2 km from the study site) and are good representatives of the overall community. Four of the trees were upper canopy with direct sunlight exposure; *E. cyathiformis* was a mid-canopy tree that receives mostly indirect sunlight. For plant hydraulic measurements, additional 12 individuals, 16 individuals at total (three to five per species), were sampled as described below.

(i) Leaf water potential

Leaf water potential (Ψ_{leaf}) was measured using a Scholander pressure chamber (PMS, Corvallis, OR, USA; accurate to 0.05 MPa; [33]). One sun leaf per study tree was collected hourly from 6.00 to 18.00 and Ψ_{leaf} measurements were made as soon as the leaf was cut from the branch. The leaves were always collected from the same height (20 ± 5 m). The Ψ_{leaf} measurements were carried out once a month from July 2015 to July 2017, characterizing the Ψ_{leaf} variation during and after the 2015–2016 El Niño.

(ii) Pressure–volume curves

The measurements were carried out from November to December 2015. Three small branches (approx. 1 m length) from each studied tree were harvested in the late afternoon, submerged in tap water and placed in a dark room to encourage overnight hydration. PV curves of 10 leaves per tree species were generated the next morning using bench drying and repeat pressurization methods [34–36]. As the leaves dried out, together with Ψ_{leaf}, leaf mass was determined from the average of three leaves with the precision of ±0.1 mg. Complete leaf PV curves were generated after 3–8 h of dehydration period. Dry mass was determined after 72 h at 70°C. Points on the PV curve that were indicative of over hydration (so-called plateau effects) were identified and corrected as suggested by Kubiske & Abrams [37]. Species turgor loss point (π_{tlp}) was calculated using the measured PV curves as described in Koide *et al.* [38]. Although π_{tlp} has been shown to vary through time, our sampling was at the peak of the drought. Therefore, the π_{tlp} measured in this study probably represents the extreme negative π_{tlp} these species manifest.

(iii) Xylem vulnerability curves

We assessed species' xylem vulnerability to cavitation and generated xylem vulnerability curves for four of the focal species (*P. anomala*, *P. erythrochrysa*, *E. cyathiformis* and *C. longipendula*). In addition, we sampled two to four additional individuals per species (a total of three to four individuals per species) found in nearby plots. These additional trees appeared visibly healthy, had similar diameters (±5 cm in DBH) and canopy positions as

the focal tree species near K34 tower and all branches were collected from approximately 20 to 25 m height. Maximum vessel lengths were estimated from the mean maximum vessel length measured (varied from 10.5 to 48.5 cm) on a minimum of three individuals per species [39]. Xylem vulnerability to cavitation was then measured using the bench dehydration method [40] using an ultra-low-flow meter [41,42]. The xylem pressures when 50% of conductivity is lost (Ψ_{50}) and when 88% of conductivity is lost (Ψ_{88}) for each species were then determined using the fatigue-corrected PLC curves [43–45]. We followed the protocols of Pereira & Mazzafera [41] to assemble the hydraulic apparatus and determine the vulnerability curve. For more details on how the PLC curves were generated, see electronic supplementary material, methods S1.

(iv) Leaf and xylem safety margins

Leaf safety margin (SM_{leaf}) was calculated as $SM_{leaf} = \Psi_{min} - \Psi_{tlp}$, where Ψ_{min} is the minimum leaf water potential measured in a particular day and Ψ_{tlp} is the leaf water potential at turgor loss point (calculated using PV curves). Xylem safety margins (SM_{P50} and SM_{P88}) were calculated as $SM_{P50} = \Psi_{min} - \Psi_{P50}$ and $SM_{P88} = \Psi_{min} - \Psi_{P88}$, where Ψ_{P50} and Ψ_{P88} are, respectively, when 50 or 88% of the xylem hydraulic conductivity is lost.

(v) Sap velocity and whole-tree hydraulic conductance

Sap velocity measurements started in March 2015 before the 2015–2016 drought hit Central Amazon. We installed one heat ratio sap flow sensor ([46]; SFM1, ICT International) per focal tree at breast height with a 5 min measurement cycle. Throughout the experiment, we moved (approx. 2) the sensors to different locations on the stem. Tree biophysical characteristics for each tree, together with Sap Flow Tool v. 1.4.1 (ICT International/Phyto-IT), were used to calculate sap velocities from raw data downloaded from the SFM1 sap flow sensors in the field. Sap velocity was measured from March 2015 to February 2017 for the species *P. anomala*, *P. erythrochrysa*, *E. cyathiformis* and *Eschweilera* sp. Owing to field logistics and sensor availability, the sap flow measurements for *C. longipendula* were discontinued in mid-September 2015.

According to Darcy's Law, $\Delta\Psi_{leaf}$ ($\Delta\Psi_{leaf} = \Psi_{midday} - \Psi_{predawn}$) and normalized sap velocity data (Q; [47]) were used to estimate whole-tree hydraulic conductance (K_{wt}) as follows (for details, see electronic supplementary material, methods S2):

$$K_{wt} = \frac{Q}{\Delta\Psi leaf}. \tag{2.1}$$

To investigate the mechanism behind the decrease of K_{wt} and sap velocity during the drought, we calculated xylem resistance and canopy stomatal resistance. Normalized xylem resistance ($1/K_s$) was determined using per cent loss of conductivity from minimum water potential measurements and xylem vulnerability curves as follows: $K_{s[i]} = 100 - PLC_i$, where PLC_i is the per cent loss of conductivity at water potential i. The normalized value of K_s was obtained by dividing $K_{s[i]}$ to $K_{s[max]}$.

The canopy stomatal resistance was calculated using Fick's law, RH, T_{air} and T_{leaf} as follows [48,49]:

$$G_s = \frac{E}{\Delta VPD}, \tag{2.2}$$

$$\Delta VPD = (e_i * RH_i) - (e_o * RH_o) \tag{2.3}$$

and

$$e = 0.611 * 10^{7.5 * \frac{T}{237.7+T}}, \tag{2.4}$$

where E is the transpiration rate, which in steady state is equal to sap flow (Q) and ΔVPD is the vapour pressure difference in kPa between leaf substomatal chamber ($e_i * RH_i$) and atmosphere ($e_o * RH_o$). RH_i and RH_o are relative humidity, expressed as a decimal, inside (we assumed is equal to 1) and outside (air) the leaf, respectively. e_i and e_o are saturated vapour pressure in kPa inside and outside the leaf, respectively. Finally, T is either equal to canopy/leaf temperature (to calculate e_i) or air temperature (when calculating e_o) and is expressed in degrees celsius.

(c) Environmental variables

(i) Vapour pressure deficit

A set of thermohygrometers (HC2S3, Campbell Scientific, Logan, UT, USA) were deployed at several heights along the K34 tower, above and beneath the canopy [29]. Air relative humidity and temperature, used to calculate VPD, at 28–35 m height were measured every 60 s and recorded as 30 min averages. Computation of VPD was performed following the Clausius–Clapeyron equation. This dataset was provided by the LBA experiment. Thirty minutes averages of VPD were used in all the analyses.

(ii) Leaf, canopy and air temperature

Leaf temperature was assessed at the peak of the El Niño (September 2015) with an NIST calibrated thermal imaging camera (FLIR-E5, Omega Engineering, 160 × 120 IR resolution; 2% accuracy). Photos were taken hourly (6.00–18.00) at a distance of 1 m just prior to leaf removal for Ψ_{leaf}. To measure canopy surface temperature (T_{canopy}), five infrared radiometer sensors (SI-111 and SI-131, Apogee) with an ultra-narrow field of view (14° half-angle; approximate view area of 0.2 m^2) were installed approximately 20 cm from the target branch on the K34 tower at 21.8, 22.8, 24.0, 25.3 and 28.8 m height. Five-minute averages of crown temperature were recorded on a data logger (CR-3000 Campbell Scientific®) for the SI-111 analogical sensors and EM-50 Decagon® for the SI-131 digital sensors). Five-minute average data were used for all the analysis. In addition, we used the AIRS (Atmospheric Infrared Sounder 1° of resolution) surface air temperature data (AIRS3STM V6, available at giovanni.gsfs.nasa.gov) centred on the Amazon field site to assess long-term series of surface air temperature before, during and after the 2015–2016 El Niño.

(iii) Precipitation, soil moisture and water table depth

Monthly rainfall data, from 2002 to 2016, were provided by the LBA hydrology group. Most of the data used in this study come from the T7 pluviometer, located at the K34 tower. When data from T7 were not available, data from the S1 pluviometer located approximately 3 km away from the K34 tower were used. The LBA hydrology group also contributed with monthly soil moisture (approx. 150 m from the K34 tower) and water table depth (approx. 500 m from the K34) data from January 2014 to April 2016 (electronic supplementary material, table S1). This dataset has soil moisture information until 300 cm depth. However, the days/times of data collection did not overlap with the water potential measurements. Therefore, we were not able to run time-stamp analyses with this dataset, and we only used it to characterize the fluctuations of volumetric soil water in the first 300 cm of the soil during the drought event. To perform coordinated and time-stamp analyses, we had an additional dataset where daily volumetric soil water content (VWC) was measured every 30 min, from September 2015 to July 2017. These measurements were performed with a Water Content Reflectometer (CS655 Campbell Scientific, Logan, UT, USA) located approximately 12 m from the K34 tower. VWC was measured at five soil's depths: 10, 20, 40, 60 and 100 cm. Soil water storage (SWS in cm) in the first 100 cm of the soil was calculated using the formula:

$$SWS = \sum_{i=1}^{n} \theta_{i,t} * \Delta Z, \tag{2.5}$$

where n is the number of layers in the soil profile, $\theta_{i,t}$ is the volumetric water content in layer i at time t and ΔZ is the depth increment from layer i to $i + 1$.

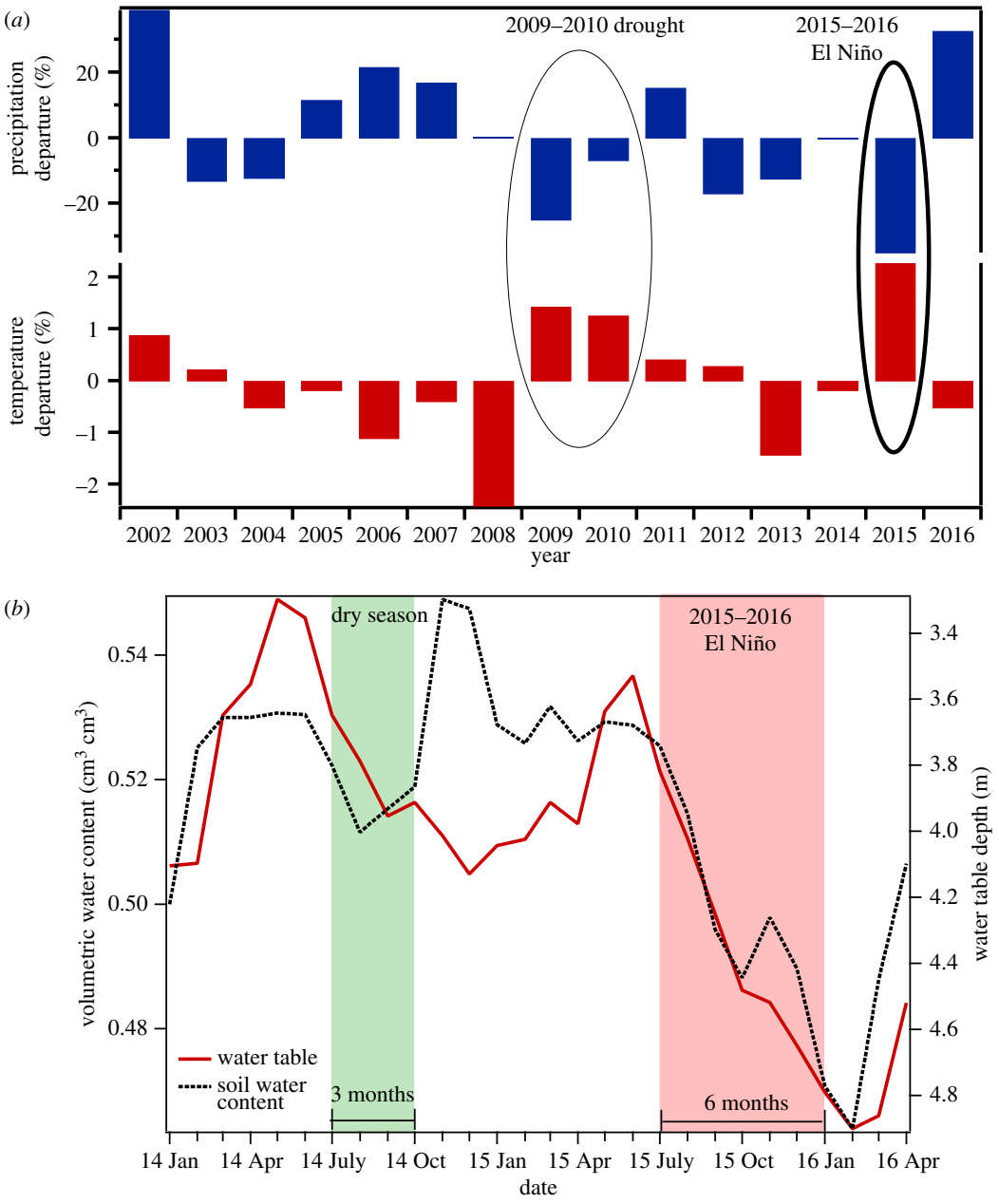

Figure 1. (*a*) Precipitation and surface air temperature departure from the long-term monthly mean (2002–2016) for the period of August–December at the K34 tower. (*b*) Volumetric water content (cm^3 cm^{-3}; VWC) in the first 3 m of the soil (black dotted lines) and water table depth (m; WTD; red solid lines) during January 2014 to April 2016. VWC and WTD were measured, respectively, approximately 150 m and approximately 500 m from the K34 tower. VWC and WTD have a sharp decrease during the El Niño (red box) compared with the previous dry season of 2014 (green box). (Online version in colour.)

(d) Statistical analyses

We used linear mixed-effect models (individual trees as random effects) to evaluate the relationship between VPD, canopy temperature and SWS and plant's SM. For these analyses, we tested four models, Model 1: all species share the same slope and intercept; Model 2: the species have different intercepts but the same slope; Model 3: species have different slopes but the same intercept and Model 4: species can have different intercepts and slopes. We report the results of the models with the lowest AIC value. To test which environmental variables, VPD or SWS, best explained species' safety margin values, we compared three models, Model VPD: VPD as the only independent variable, Model SWS: SWS as the only independent variable and Model VPD + SWS: VPD and SWS as the independent variables. Analysis of covariance (ANCOVA) with a random species effect was used to assess the relationship between sap velocity before and during the 2015–2016 El Niño and VPD, and between sap velocity and SWS during and after the drought. All models were implemented in R v. 3.0.2 (R Development Core Team, 2013).

3. Results

(a) Record-breaking high temperatures and high vapour pressure deficits were observed during the 2015–2016 drought

During previous droughts (e.g. 2009–2010), high temperatures or low precipitation were observed (figure 1). However, during the 2015–2016 El Niño, higher temperatures (2% or 1.2°C higher) and lower precipitation (approx. 25% or 31 mm lower) for the months of August–December, compared to the long-term average, were recorded (figure 1*a*). In particular, a 20% (22.8 mm) reduction in precipitation was observed during August–December 2015 relative to the same period in 2010 (electronic supplementary material, figure S1), and thus 2015 may be the hottest year in Amazonia in the last 100 years [7].

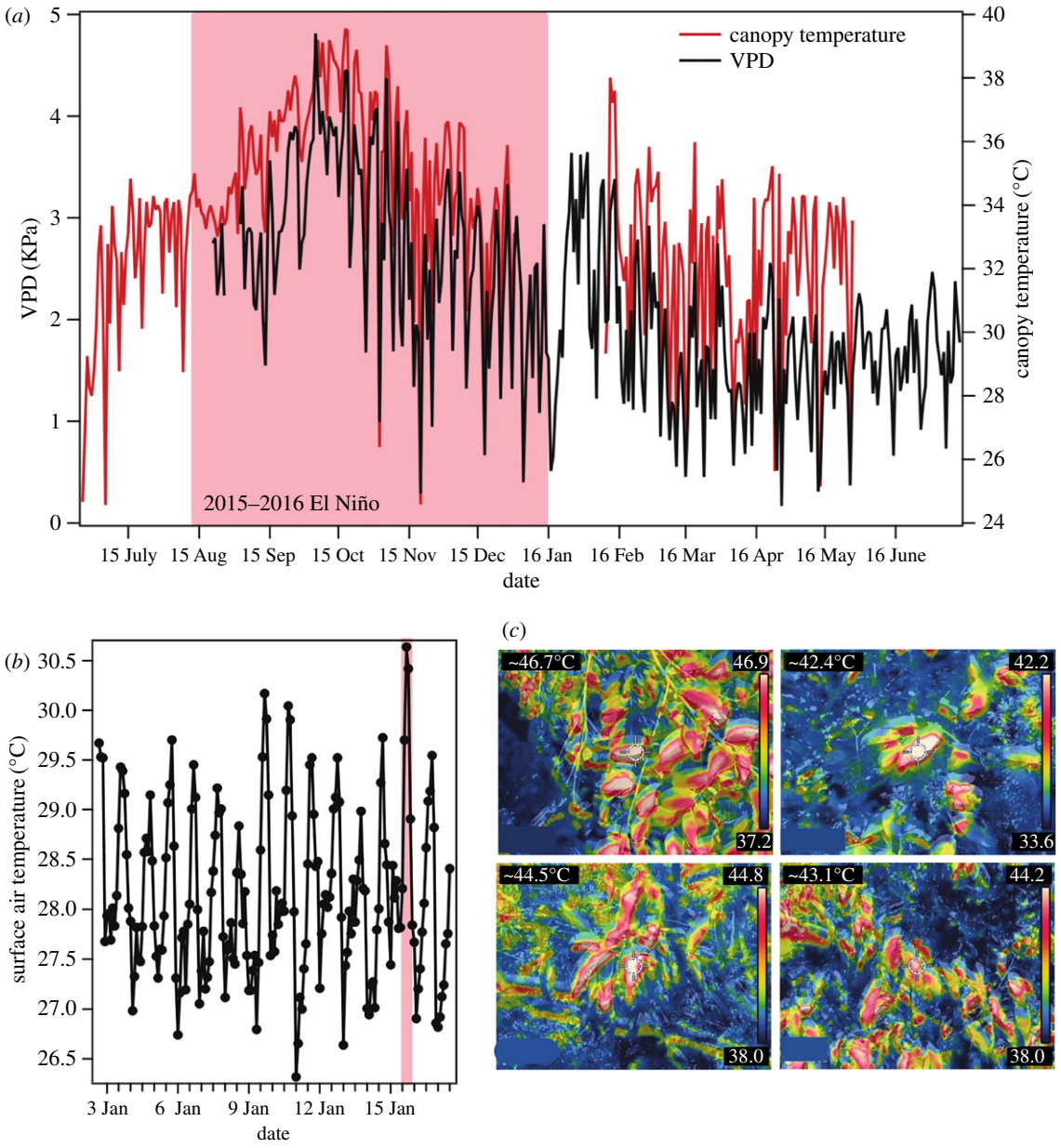

Figure 2. (*a*) Daily maximum VPD (black line) and canopy temperature (T_{canopy}; red line) at the K34 tower from July 2015 to June 2016. (*b*) Landscape scale monthly averaged air surface temperatures at the study site for the period of September 2002–August 2017. (*c*) Midday thermal leaf surface temperature photos taken for each studied species during the peak of the El Niño (September 2015). The red box represents the 2015–2016 El Niño.

The record low in precipitation during the 2015–2016 El Niño contributed to approximately 8% (0.2 cm^3 cm^3) and 11% (2.12 m) lower VWC and water table depth, respectively, in relation to the dry season of 2014 (figure 1*b*). However, the absolute changes in soil water content in the first 3 m of the soil were small, suggesting that water supply for plants was not very limited during the study period.

Satellite observations revealed that September 2015 exhibited the warmest monthly averaged surface air temperature of any other month over the past 13 years at the study site (figure 2*b*). Daytime air temperatures in September were nearly 1.0°C warmer than any month from other dry years (2005 and 2010). A maximum daytime canopy temperature of upper canopy leaves increased 5–7°C during the drought compared to the pre-drought period (figure 2*a*). Furthermore, during the peak of the El Niño (September 2015), individual sun-exposed leaf temperatures of the study trees reached approximately 47 ± 1°C, almost 10°C higher than the maximum canopy temperature registered in that month (figure 2*a*,*c*). Owing to an increase in air temperature and a decrease in air relative humidity, VPD also increased in the El Niño months (figure 2*a*), reaching approximately 5 kPa during the day and 1 kPa during the night (in September 2015), 40% and 95% higher, respectively, then after the drought (figure 2*a*).

H1: Species' leaf and xylem hydraulic safety margins will narrow with an increase in vapour pressure deficit or decrease in soil water supply.

We analysed leaf and xylem SM (SM_{leaf} and $SM_{P50,88}$, respectively) during and after the 2015–2016 El Niño to determine the sensitivity of plants to VPD and SWS. Daily minimum leaf water potential (Ψ_{min}) measurements throughout the drought (August–December 2015) were significantly different (paired-sample *t*-test: *p*-value $= 7.179 \times 10^{-5}$) and up to 1.9 MPa (59%) more negative than during the same period in 2016 (figure 3). Even though we found a high variation in species response to the drought (figure 3; electronic

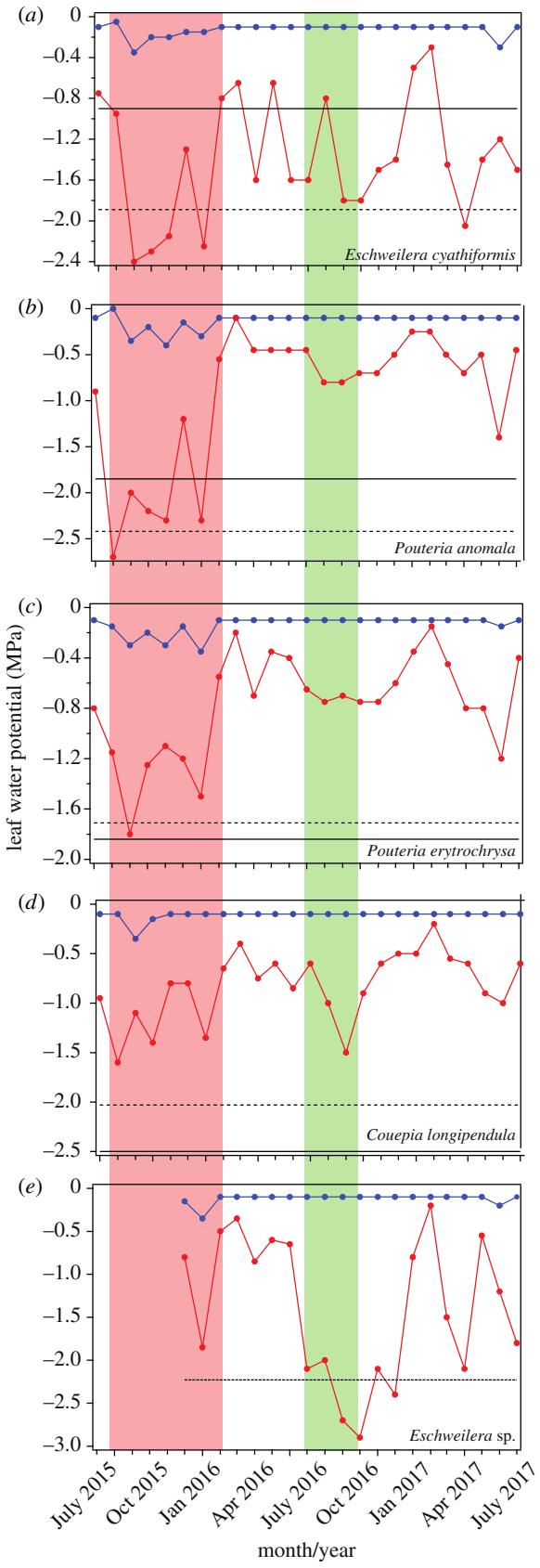

Figure 3. Two years of monthly predawn (blue line) and daily minimum (red line) leaf water potential (July 2015–2017), leaf turgor loss point (dashed black line), 50% loss of hydraulic conductivity (P_{50}; solid black line) for five Amazonian tree species at the K34 tower. The red and green boxes represent the 2015–2016 El Niño and the regular 2016 dry season, respectively.

supplementary material, figure S2), plant's SMs, regardless of species, were highly sensitive to changes in VPD (figure 4) and T_{Canopy} (electronic supplementary material, figure S3). An increase of 1 kPa in VPD caused a decrease of 0.43 and 0.34 MPa in SM_{leaf} and SM_{P50}, respectively (electronic supplementary material, table S2). Applying a more conservative xylem safety margin (SM_{P88}) showed a similar relationship between SM and VPD (figure 4*c*).

On the other hand, the relationship between SM_{leaf}, SM_{P88} and SWS was non-significant ($p = 0.842$ and 0.171, respectively). The relationship between SM_{P50} and SWS was weak (estimate $= -0.13$ and $p = 0.0378$), and species had statistically similar slopes but random intercepts (electronic supplementary material, table S3). In addition, when comparing the models used to test the effect of VPD, SWS and VPD + SWS on trees' SMs, only Model VPD was statistically significant ($p = 0.005$; electronic supplementary material, table S4). Furthermore, predawn measurements during the drought were high (approx. 0.3 MPa; figure 3) and had a weak relationship with SWS (electronic supplementary material, figure S4 and table S5), suggesting that soil water availability was not limiting during our study period. These results indicate that atmospheric demand but not superficial soil water supply was driving the decrease in plants' SMs observed during our study period.

H2: The decline in sap velocity during the drought will be mainly explained by a decrease in whole-tree hydraulic conductance caused by increased xylem resistance due to a spread in xylem embolism.

Sap velocity and whole-tree hydraulic conductance (K_{wt}) during the peak of the 2015–2016 drought had an approximately 35 and 70% reduction, respectively, compared to values recorded before and after the El Niño (figure 5). The decline in sap velocity was correlated with an increase in VPD, but had a weak correlation with SWS (figure 6*a*,*b*; electronic supplementary material, table S6), corroborating our findings that atmospheric demand had a greater impact on plant's physiological performance than water supply during our study period. Furthermore, species that substantially crossed their P_{50} during the El Niño (e.g. *E. cyathiformis*) were not able to completely recover sap velocity to pre-drought values (figures 3 and 5), indicating that the drought caused permanent damage to species' xylem. Finally, based on our calculations of canopy stomatal ($1/G_s$) and xylem ($1/K_s$) resistances, the decrease in sap velocity was due to a combination of xylem cavitation and stomatal closure (figure 7*a*–*c*). Therefore, we reject our hypothesis that the decrease in sap velocity and K_{wt} was mainly explained by an increase in xylem cavitation.

4. Discussion

This study reveals how leaf water relations and xylem transport characteristics in five Amazonian trees species responded to a severe hot and dry climate event, and whether these responses were related to an increase in VPD, a decrease in SWS and xylem embolism formation. The studied trees showed great sensitivity to unusually high canopy temperatures and VPD but not to superficial soil water content. Moreover, during the El Niño, due to a high atmospheric demand, tree transpiration declined. Finally, despite the stomatal closure, the studied trees showed increased xylem embolism that affected their ability to transport water to tree crowns under the warmer and drier El Niño conditions.

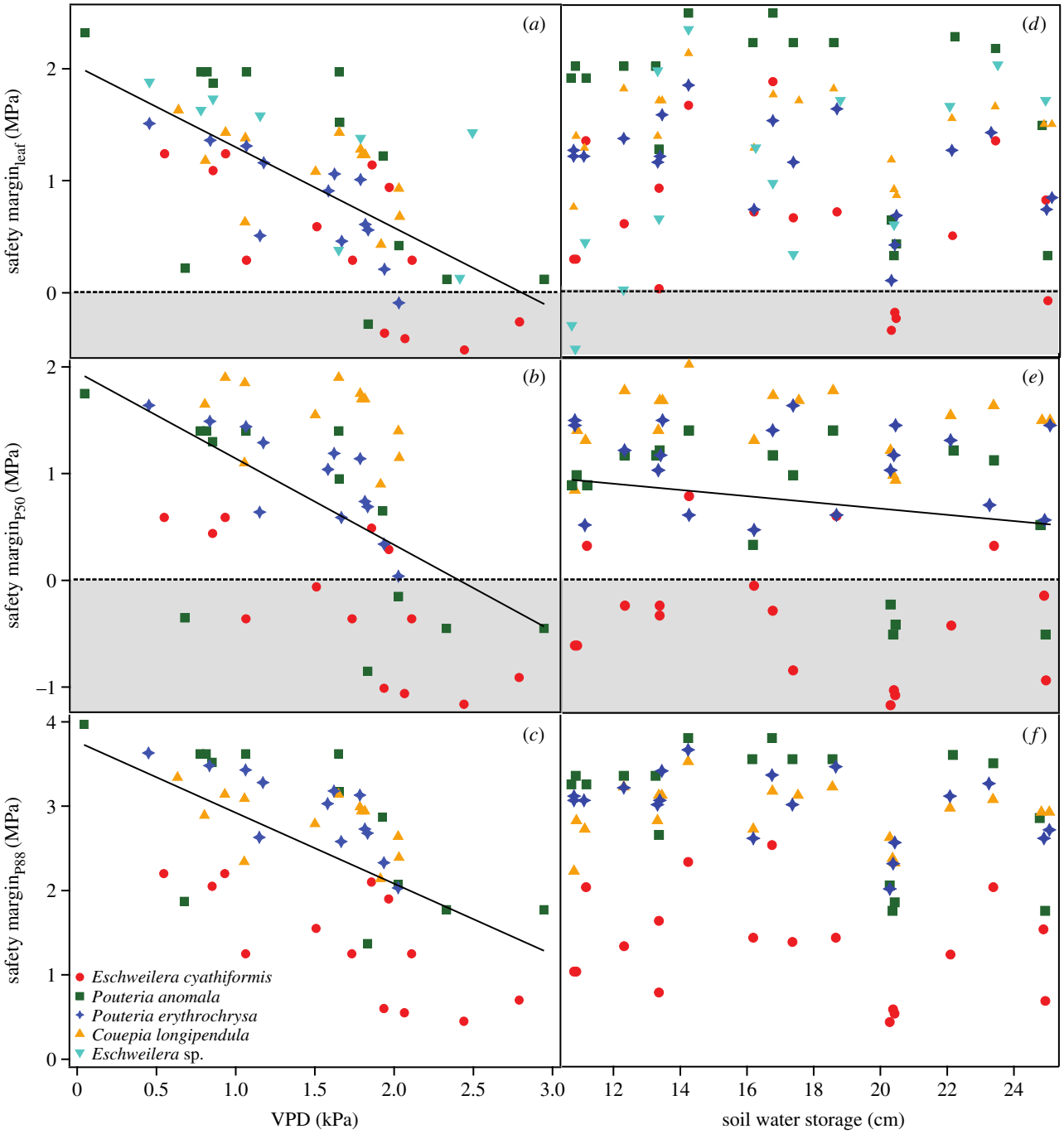

Figure 4. The relationship between (*a–c*) leaf and xylem SM and VPD ($n = 52–60$) in kPa—species had statistically different intercepts but similar slope, *p*-value ranged from 1.17×10^{-8} to 6.24×10^{-5}; and (*d–f*) leaf and xylem SM and SWS ($n = 74–89$) in cm—the only statistically significant relationship ($p = 0.0378$) was SM_{P50} versus SWS, where species had random intercepts but the same slope; for five Amazonian tree species at K34 tower. Where leaf safety margin (SM_{leaf}) = $\Psi_{tlp} - \Psi_{min}$; tlp = leaf turgor loss point; xylem safety margin P_{50} (SM_{P50}) = $\Psi_{50} - \Psi_{min}$; xylem safety margin P_{88} (SM_{P88}) = $\Psi_{80} - \Psi_{min}$. The black lines indicate the relationship between SM and canopy temperature without considering species identity. A summary of the statistical results from the best models (lowest AIC values) can be found in electronic supplementary material, tables S3 and S4.

(a) Effects of the 2015–2016 drought on local climatic variables

The precipitation and soil water data in the central Amazon (figure 1) indicate that the 2015–2016 El Niño was the most severe drought seen in the last decade, surpassing the so-called once in a century droughts of 2005 and 2010 [7,50,51]. Along with the very low water supply, the atmospheric demand for water from the forests also increased (figure 2). The long-term air temperature data corroborate the findings that 2015–2016 El Niño contributed to the hottest year in the last decade [7]. Leaf temperatures were also record-breaking, reaching values (approx. 47°C; figure 2) that have been shown to denature leaf proteins such as Rubisco, and cause oxidative damage to photosynthetic structures [52]. VPD was also considerably higher (approx. 40–95%) during the drought than after the El Niño (figure 2), exacerbating physiological stress on plants by increasing plant water loss and reducing net carbon uptake [15]. Our results, showing the physiological responses of five Amazonian trees to this novel and extremely hot and dry conditions, provides an important example of how trees may be impacted by future climatic events.

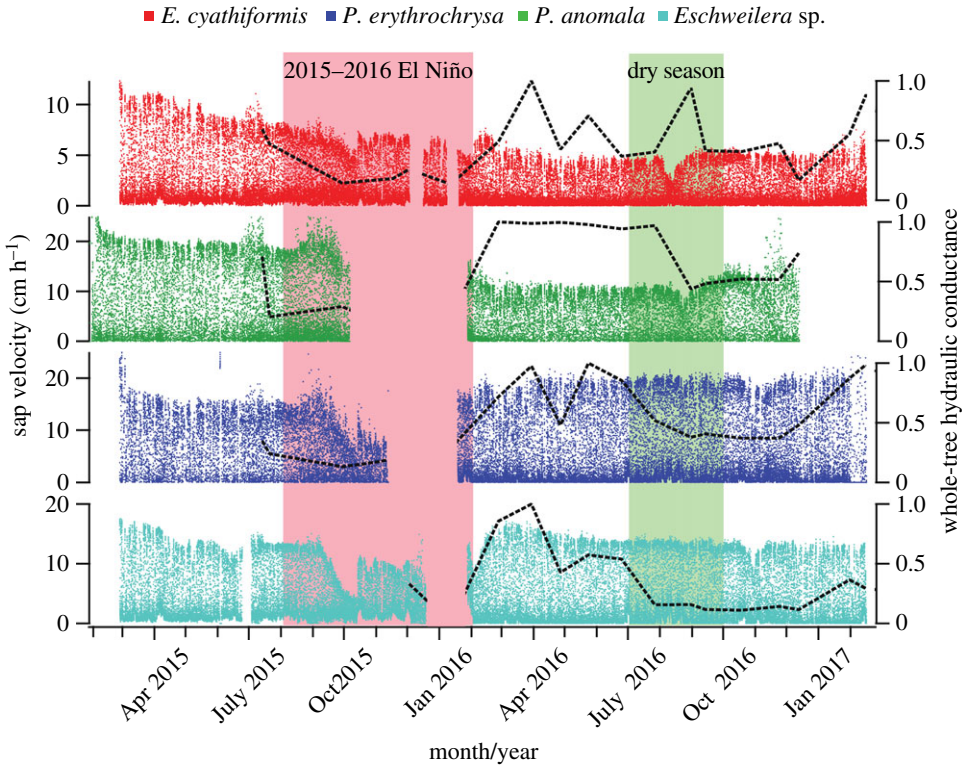

Figure 5. Response and recovery of four Amazonian tree species to the 2015–2016 El Niño in terms of sap velocity (measurements recorded every 5 min) and normalized whole-tree hydraulic conductance ($K_{wt}/K_{wt[max]}$; black dashed line). The red and green boxes represent the duration of the 2015–2016 El Niño and the 2016 dry season, respectively. Data gaps represent periods where continuous power was not available and sap velocity could not be measured.

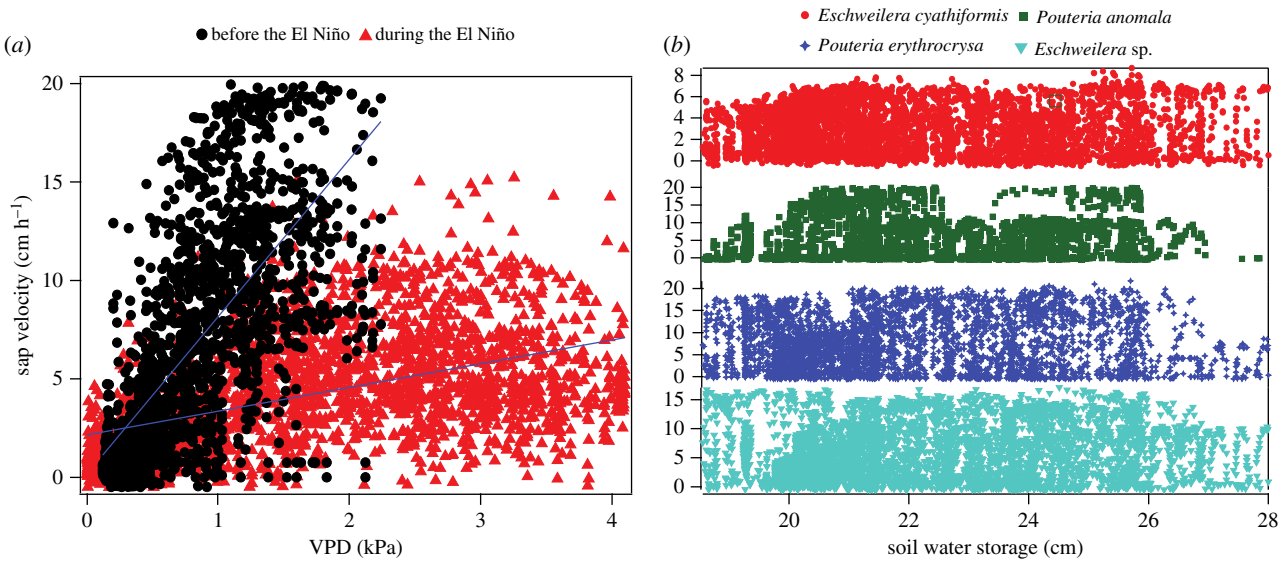

Figure 6. The relationship between (*a*) sap velocity and VPD—a significantly different slope and intercept are observed before (black circles; May and June 2015) and during the peak of the El Niño (red triangles; October 2015) and (*b*) sap velocity and SWS in the first 1 m, during and before the El Niño (September 2015–May 2016), for four Amazonian tree species. The relationship between sap velocity and SWS was not significantly different, and species had different intercepts and slopes from each other. Summary of the statistical results can be found in electronic supplementary material, table S6.

H1: Species' leaf and xylem hydraulic safety margins will narrow with an increase in vapour pressure deficit or decrease soil water supply.

A significantly negative relationship between leaf (SM_{leaf}) and xylem (SM_{P50} and SM_{P88}) SM and VPD was found (figure 4), indicating that plants' live and dead tissues are both sensitive to an increase in temperature and VPD. In addition, the high temperatures recorded during the drought, coupled with low air relative humidity, caused most species to operate under negative SM (SM_{leaf} and SM_{P50}). These results suggest that future extreme warming events can be particularly stressful for some Amazonian trees and corroborate findings that warmer temperatures greatly amplify tree's stress and potentially mortality [5,8,9,13].

Interestingly, the predawn leaf water potential ($\Psi_{predawn}$) values were high (figure 3), suggesting that soil water availability was never limiting during our study period. This interpretation is consistent with the small absolute changes in soil water content (figure 1*b*) in the first 300 cm of the soil, and with the weak relationship found between SM_{P50} and SWS (figure 4*d–f*) and

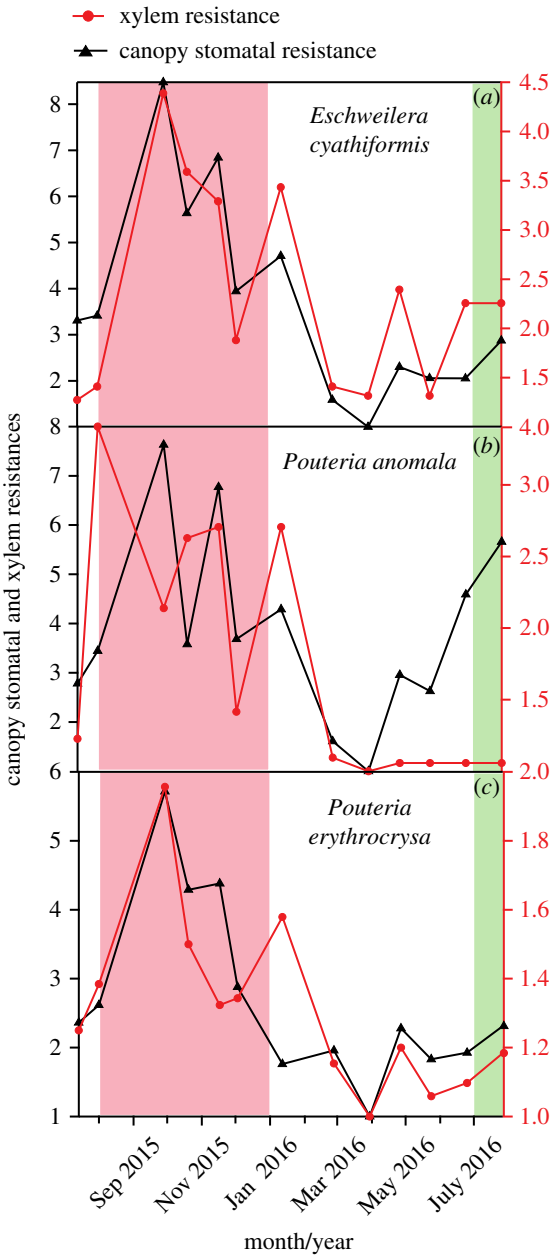

Figure 7. (*a–c*) Variations in canopy stomatal resistance ($1/G_s$; black rectangles) and xylem resistance ($1/K_s$; red circles) during July 2015 to July 2017 for three central Amazonian trees. G_s and K_s are normalized values ($G_{s[i]} = G_{s[j]}/G_{s[max]}$ and $K_{s[i]} = K_{s[j]}/K_{s[max]}$, respectively) and does not have units. The red and green boxes represent the 2015–2016 El Niño and 2016 dry season, respectively.

sap velocity and SWS in the first 100 cm of the soil (figure 6*b*). As concluded by a previous study at the same site, more than 40% of the total demand for transpiration is supplied by the first 100 cm of the soil, whereas the first 300 cm contributed with approximately 76% (2.03 mm d^{-1}) [53]. However, they noted that during drought events, plant water uptake occurred below 480 cm, suggesting that these trees might rely on deeper soil water during extremely dry years. A recent study conducted in a seasonal Amazonian forest found a niche segregation of root water uptake in the soil, allowing multi-species coexistence in that forest [54]. Therefore, we cannot exclude the possibility that the studied trees are using deep water to survive extreme droughts and future studies should investigate the relationship between SWS and SMs along a deeper soil profile. Nonetheless, the studied trees were still operating under negative SMs during the drought (figure 4), indicating that the atmospheric water demand was higher than the water supply causing these trees to experience low xylem tensions during the day.

Xylem SM can be defined in different ways [55,56]. Here, we used two safety margin metrics: SM_{P50} ($\Psi_{min} - \Psi_{50}$), which is the most widely used, and SM_{P88} ($\Psi_{min} - \Psi_{88}$), which is a more conservative safety margin calculation. While negative values of SM_{P50} were recorded during the 2015–2016 drought, SM_{P88} narrowed but were always positive (figure 4). In addition, none of the studied trees died during the 2015–2016 El Niño and were still alive in 2017 (tree mortality of other trees nearby was not evident either), supporting the findings that, for angiosperms, the lethal level of cavitation is close to 88% of embolized vessels (although this still has not been tested in Amazonian trees; [28,57–59]). Furthermore, during our 2 years of Ψ_{leaf} measurements (figure 3), we did not register SM_{P50} greater than 1.7 MPa (figure 4). These results support the conclusion that most trees operate close to their cavitation threshold [27], probably because narrow SMs maximize gas exchange while avoiding hydraulic failure [60].

The extreme climatic conditions imposed by the El Niño, caused some trees to cross leaf π_{tlp}, suggesting that leaf tissues were also under water stress. The loss of leaf turgor pressure causes leaf wilting resulting in complete stomatal closure [19,36,61]. Our results corroborate other findings that plants can sustain low Ψ_{leaf} for a substantial amount of time and still recover after a re-hydration period [62]. The high $\Psi_{predawn}$ values (figure 3) suggest that even though plants crossed their π_{tlp} during the day, they were able to re-hydrate at least some of their leaf tissues during the night (through stomatal closure) preventing tree death. Furthermore, when leaf temperature reaches 37–50°C, which was the case during the 2015–2016 drought (figure 2), leaf proteins start to denature, and carbon assimilation processes are impaired [52,63]. High leaf temperatures are well known to stimulate the overproduction of reactive oxidative species (ROS; [64]), triggering programmed cell death under excessive ROS accumulation [65]. These findings help explain the many upper canopy wilted and heat damaged leaves observed in the field during the drought. About half of them were able to recover, and the other half dried out and could not regain function.

H2: The decline in sap velocity during the drought will be mainly explained by a decrease in whole-tree hydraulic conductance caused by increased xylem resistance due to a spread in xylem embolism.

As canopy temperature and VPD during the El Niño continued to increase, sap velocity and whole-tree hydraulic conductance (K_{wt}) showed a significant decline (figure 5). Under a severe drought, plants can (i) close their stomata to reduce water loss through transpiration, at the cost of carbon assimilation and leaf cooling, (ii) leave stomata open (or partially open) and allow xylem tension to increase, risking the integrity of their hydraulic system and (iii) can drop all or most of their leaves to prevent further water loss [55,66,67]. All of these three strategies could cause sap velocity (SV) and K_{wt} to decrease; however, during our study period, we did not observe significant leaf loss that may explain the drop in SV (K Jardine, BO Gimenez 2018, personal communications). Therefore, we only considered stomatal resistance and xylem resistance (embolism formation) in our analyses.

To investigate the processes behind the reduction in sap velocity and K_{wt} in our studied trees, we calculated the canopy stomatal ($1/G_s$) and xylem resistances ($1/K_s$) during and after the El Niño. We found that species that crossed their P_{50}

(*E. cyathiformis* and *P. anomala*) had high values of $1/K_s$. Canopy stomatal resistance was also high during the El Niño and decreased after the drought. These results suggest that as xylem tension increased and vessels experienced cavitation, plants downregulated stomatal conductance but were unable to completely prevent xylem embolism. Also, for most of the studied trees, a decline in sap velocity was also observed after individuals reached their P_{50} and did not go up again to pre-drought values, even when a recovery in precipitation occurred (figure 5). If only a small portion of the xylem embolizes, the upward movement of water in the tree may continue with minor impact on plant performance [24]. However, widespread embolism in the xylem, like we report in this study, forces trees to operate with less functional xylem, reducing trees' capacity to transport water from the soil to leaves [66,68], and as a consequence, a decrease in sap velocity and K_{wt} is observed. These findings indicate that daily cavitation and embolism refilling under tension is not routine for these Amazonian trees. Drought-induced xylem cavitation is thus a symptom of distress, and plants would have to rely on the growth of new vessels to continue to transport water [28,69,70].

However, if some of the studied trees were experiencing a dangerous increase in xylem tension, why were they not able to completely close their stomata to prevent further increase in xylem cavitation? A reasonable explanation is that the studied trees may lack the ability to respond rapidly to conserve water during severe droughts. Plants growing in environments where drought events are recurring usually exhibit rapid stomatal responses to water deficit [60,71]. However, wet tropical forests are thermally stable, and large fluctuations in water supply and demand do not frequently occur. Most Amazonian plants may not need to rely on drought-resistance hydraulic strategies to survive drier conditions, because water generally does not represent a limiting resource in rainforest ecosystems [13,17]. Therefore, the ability of Amazonian trees to survive future climatic events may depend on how well they will be able to acclimate to hotter and drier conditions [13]. Another explanation may be the maintenance of transpiration as a leaf thermoregulatory mechanism [72]. These trees may be favouring to assume hydraulic risks instead of damaging their photosynthetic apparatus. These would be particularly beneficial if trees were able to recover from xylem cavitation; however, the ability of plants to refill embolized vessel is still questionable [73].

Although our sample size was limited due to logistical constraints, we report the longest record of diurnal leaf water potential measurements for Amazonian trees to date. We assessed stem and leaf hydraulic response to an extreme climate-change type of drought and demonstrated that five focal Amazonian species are susceptible to climate warming. We would like to point out that our results hold true for the five individual tree species sampled in this study and more research on the impact of natural droughts on Amazonian trees are needed before any extrapolation is made. Furthermore, linking drought stress vulnerability, with VPD and leaf temperature, can strengthen the current understanding of plant function and facilitate the identification of relationships indicative of ecosystem sensitivity or tolerance to drought. Therefore, studies like ours that measure *in situ* trees' response to a severe drought event are vital if we are to predict what will happen to plant communities under a warmer and drier climate.

Data accessibility. The precipitation, air temperature and relative humidity data are open access and can be found at the link: http://lba2.inpa.gov.br/index.php/repository/Boletins-Hidrol%C3%B3gicos/orderby,4/. The monthly soil moisture data in the first 3 m of the soil are presented in electronic supplementary material, table S1 and the raw data are available upon request to the LBA Hydrology group through the link: https://docs.google.com/forms. The daily soil moisture data of the first 1 m of the soil and our physiological data are available in the NGEE-Tropics Data Archive and can be made available upon request.

Authors' contributions. C.G.F., T.E.D., K.J.J., P.V.A.F. and J.Q.C. planned and designed the research. C.F.G., K.J.J., B.O.G. and A.C.A. performed experiments and conducted fieldwork. C.F.G., T.E.D., K.J.J., N.M., L.A., R.N.-J., N.H. and J.Q.C. analysed and interpreted data. C.F.G., T.E.D., K.J.J., N.M., B.O.G., L.A., R.N.-J., P.V.A.F. and J.Q.C. wrote the manuscript. All authors gave final approval for publication.

Competing interests. We declare we have no competing interests.

Funding. The data collection was supported as part of the *Next Generation Ecosystem Experiment-Tropics project*, funded by the U.S. Department of Energy, Office of Science, Office of Biological and Environmental Research—contract no. DE-AC02-05CH11231. C.G.F. received a Ph.D. scholarship from the *Science Without Boarders Program*—Brazil (award no. 99999.001262/2013-00), through the *Coordenação de Aperfeiçoamento de Pessoal de Nível Superior (CAPES)*. Additional funding for C.G.F and T.E.D. was provided by the University of California at Berkeley, Department of Integrative Biology through the *Research Grant*.

Acknowledgements. We thank the Forest Management Laboratory (LMF) at *Instituto Nacional de Pesquisas da Amazônia* (*INPA*) for logistical and scientific support and the *Large Scale Biosphere-Atmosphere Program (LBA)–INPA* for contributing with climatic data and logistical support. We thank the two anonymous reviewers, Robert Paul Skelton, Gabriel Damasco and all the Dawson Laboratory members for insightful feedback that enhanced the manuscript.

References

1. Mayle FE, Power MJ. 2008 Impact of a drier Early-Mid-Holocene climate upon Amazonian forests. *Phil. R. Soc. B* **363**, 1829–1838. (doi:10.1098/rstb.2007.0019)
2. Irion G, Bush M, De Mello JN, Stüben D, Neumann T, Müller G, Junk J. 2006 A multiproxy palaeoecological record of Holocene lake sediments from the Rio Tapajós, eastern Amazonia. *Palaeogeogr. Palaeoclimatol. Palaeoecol.* **240**, 523–535. (doi:10.1016/j.palaeo.2006.03.005)
3. Marengo J, Espinoza J. 2015 Extreme seasonal droughts and floods in Amazonia: causes, trends and impacts. *Int. J. Climatol.* **36**, 1033–1050. (doi:10.1002/joc.4420)
4. Jenkins H, Baker P, Guilderson T. 2010 Extreme drought events revealed in Amazon tree ring records. In *AGU Fall Meeting Abstracts*. San Francisco, CA, USA: American Geophysical Union.
5. Doughty CE *et al.* 2015 Drought impact on forest carbon dynamics and fluxes in Amazonia. *Nature* **519**, 78–82. (doi:10.1038/nature14213)
6. Stocker TF *et al.* 2013 *IPCC, 2013: climate change 2013: the physical science basis*. Contribution of working group I to the fifth assessment report of the intergovernmental panel on climate change. Cambridge, UK: Cambridge University Press.
7. Jiménez-Muñoz JC, Mattar C, Barichivich J, Santamaría-Artigas A, Takahashi K, Malhi Y, Sobrino JA, van der Schrier G. 2016 Record-breaking warming and extreme drought in the Amazon rainforest during the course of El Niño 2015–2016. *Sci. Rep.* **6**, 33130. (doi:10.1038/srep33130)
8. Trenberth KE, Dai A, Van Der Schrier G, Jones PD, Barichivich J, Briffa KR, Sheffield J. 2014 Global warming and changes in drought. *Nat. Clim. Change* **4**, 17–22. (doi:10.1038/nclimate2067)
9. Allen CD, Breshears DD, McDowell NG. 2015 On underestimation of global vulnerability to tree

mortality and forest die-off from hotter drought in the Anthropocene. *Ecosphere* **6**, 1–55. (doi:10.1890/ES15-00203.1)

10. Jung M *et al.* 2010 Recent decline in the global land evapotranspiration trend due to limited moisture supply. *Nature* **467**, 951–954. (doi:10.1038/nature09396)
11. Eamus D, Boulain N, Cleverly J, Breshears DD. 2013 Global change-type drought-induced tree mortality: vapor pressure deficit is more important than temperature per se in causing decline in tree health. *Ecol. Evol.* **3**, 2711–2729. (doi:10.1002/ece3.664)
12. Will RE, Wilson SM, Zou CB, Hennessey TC. 2013 Increased vapor pressure deficit due to higher temperature leads to greater transpiration and faster mortality during drought for tree seedlings common to the forest–grassland ecotone. *New Phytol.* **200**, 366–374. (doi:10.1111/nph.12321)
13. Doughty CE, Goulden ML. 2008 Are tropical forests near a high temperature threshold? *J. Geophys. Res. Biogeosci.* **113**, 1–12. (doi:10.1029/2007JG000632)
14. Anderegg WR, Anderegg LD, Berry JA, Field CB. 2014 Loss of whole-tree hydraulic conductance during severe drought and multi-year forest die-off. *Oecologia* **175**, 11–23. (doi:10.1007/s00442-013-2875-5)
15. McDowell N *et al.* 2008 Mechanisms of plant survival and mortality during drought: why do some plants survive while others succumb to drought? *New Phytol.* **178**, 719–739. (doi:10.1111/j.1469-8137.2008.02436.x)
16. Anderegg LD, Anderegg WR, Abatzoglou J, Hausladen AM, Berry JA. 2013 Drought characteristics' role in widespread aspen forest mortality across Colorado, USA. *Glob. Change Biol.* **19**, 1526–1537. (doi:10.1111/gcb.12146)
17. Janzen DH. 1967 Why mountain passes are higher in the tropics. *Am. Nat.* **101**, 233–249. (doi:10.1086/282487)
18. Gleason SM *et al.* 2016 Weak tradeoff between xylem safety and xylem-specific hydraulic efficiency across the world's woody plant species. *New Phytol.* **209**, 123–136. (doi:10.1111/nph.13646)
19. Bartlett MK, Scoffoni C, Sack L. 2012 The determinants of leaf turgor loss point and prediction of drought tolerance of species and biomes: a global meta-analysis. *Ecol. Lett.* **15**, 393–405. (doi:10.1111/j.1461-0248.2012.01751.x)
20. Powell TL, Wheeler JK, de Oliveira AA, da Costa L, Carlos A, Saleska SR, Meir P, Moorcroft PR. 2017 Differences in xylem and leaf hydraulic traits explain differences in drought tolerance among mature Amazon rainforest trees. *Glob. Change Biol.* **23**, 4280–4293. (doi:10.1111/gcb.13731)
21. Oliveira RS. 2013 Can hydraulic traits be used to predict sensitivity of drought-prone forests to crown decline and tree mortality? *Plant Soil* **364**, 1–3. (doi:10.1007/s11104-012-1508-9)
22. Binks O *et al.* 2016 Plasticity in leaf-level water relations of tropical rainforest trees in response to experimental drought. *New Phytol.* **211**, 477–488. (doi:10.1111/nph.13927)
23. Maréchaux I, Bartlett MK, Sack L, Baraloto C, Engel J, Joetzjer E, Chave J. 2015 Drought tolerance as predicted by leaf water potential at turgor loss point varies strongly across species within an Amazonian forest. *Funct. Ecol.* **29**, 1268–1277. (doi:10.1111/1365-2435.12452)
24. Tyree MT, Sperry JS. 1989 Vulnerability of xylem to cavitation and embolism. *Annu. Rev. Plant Biol.* **40**, 19–36. (doi:10.1146/annurev.pp.40.060189.000315)
25. Williams CB, Reese Næsborg R, Dawson TE. 2017 Coping with gravity: the foliar water relations of giant sequoia. *Tree Physiol.* **37**, 1312–1326. (doi:10.1093/treephys/tpx074)
26. Trifilò P, Nardini A, Gullo MAL, Barbera PM, Savi T, Raimondo F. 2015 Diurnal changes in embolism rate in nine dry forest trees: relationships with species-specific xylem vulnerability, hydraulic strategy and wood traits. *Tree Physiol.* **35**, 694–705. (doi:10.1093/treephys/tpv049)
27. Choat B *et al.* 2012 Global convergence in the vulnerability of forests to drought. *Nature* **491**, 752–755. (doi:10.1038/nature11688)
28. Delzon S, Cochard H. 2014 Recent advances in tree hydraulics highlight the ecological significance of the hydraulic safety margin. *New Phytol.* **203**, 355–358. (doi:10.1111/nph.12798)
29. Araújo A *et al.* 2002 Comparative measurements of carbon dioxide fluxes from two nearby towers in a central Amazonian rainforest: the Manaus LBA site. *J. Geophys. Res. Atmos.* **107**, 58. (doi:10.1029/2001JD000676)
30. Sombroek W. 2001 Spatial and temporal patterns of Amazon rainfall. Consequences for the planning of agricultural occupation and the protection of primary forests. *Ambio* **30**, 388–396. (doi:10.1579/0044-7447-30.7.388)
31. Higuchi N, Santos J, Lima A, Higuchi F, Chambers JQ. 2011 A floresta Amazônica e a água da chuva. *FLORESTA* **41**, 417–434. (doi:10.5380/rf.v41i3.24060)
32. Luizão RC, Luizão FJ, Paiva RQ, Monteiro TF, Sousa LS, Kruijt B. 2004 Variation of carbon and nitrogen cycling processes along a topographic gradient in a central Amazonian forest. *Glob. Change Biol.* **10**, 592–600. (doi:10.1111/j.1529-8817.2003.00757.x)
33. Scholander PF, Hammel H, Bradstreet ED, Hemmingsen E. 1965 Sap pressure in vascular plants. *Science* **148**, 339–346. (doi:10.1126/science.148.3668.339)
34. Tyree M, Hammel H. 1972 The measurement of the turgor pressure and the water relations of plants by the pressure-bomb technique. *J. Exp. Bot.* **23**, 267–282. (doi:10.1093/jxb/23.1.267)
35. Hinckley T, Duhme F, Hinckley A, Richter H. 1980 Water relations of drought hardy shrubs: osmotic potential and stomatal reactivity. *Plant Cell Environ.* **3**, 131–140.
36. Sack L, Cowan P, Jaikumar N, Holbrook N. 2003 The 'hydrology' of leaves: co-ordination of structure and function in temperate woody species. *Plant Cell Environ.* **26**, 1343–1356. (doi:10.1046/j.0016-8025.2003.01058.x)
37. Kubiske M, Abrams M. 1991 Rehydration effects on pressure-volume relationships in four temperate woody species: variability with site, time of season and drought conditions. *Oecologia* **85**, 537–542. (doi:10.1007/BF00323766)
38. Koide RT, Robichaux RH, Morse SR, Smith CM. 1989 Plant water status, hydraulic resistance and capacitance. In *Plant physiological ecology* (eds H Lambers, FS Chapin III, TL Pons), pp. 161–183. Berlin, Germany: Springer.
39. Jacobsen AL, Pratt RB, Ewers FW, Davis SD. 2007 Cavitation resistance among 26 chaparral species of Southern California. *Ecol Monogr.* **77**, 99–115. (doi:10.1890/05-1879)
40. Sperry J, Donnelly J, Tyree M. 1988 A method for measuring hydraulic conductivity and embolism in xylem. *Plant Cell Environ.* **11**, 35–40. (doi:10.1111/j.1365-3040.1988.tb01774.x)
41. Pereira L, Mazzafera P. 2012 A low cost apparatus for measuring the xylem hydraulic conductance in plants. *Bragantia* **71**, 583–587. (doi:10.1590/S0006-87052013005000006)
42. Pereira L, Bittencourt PR, Oliveira RS, Junior M, Barros FV, Ribeiro RV, Mazzafera P. 2016 Plant pneumatics: stem air flow is related to embolism–new perspectives on methods in plant hydraulics. *New Phytol.* **211**, 357–370. (doi:10.1111/nph.13905)
43. Hacke UG, Stiller V, Sperry JS, Pittermann J, McCulloh KA. 2001 Cavitation fatigue. Embolism and refilling cycles can weaken the cavitation resistance of xylem. *Plant Physiol.* **125**, 779–786. (doi:10.1104/pp.125.2.779)
44. Paddock III WA, Davis SD, Pratt RB, Jacobsen AL, Tobin MF, López-Portillo J, Ewers FW. 2013 Factors determining mortality of adult chaparral shrubs in an extreme drought year in California. *Aliso J. Syst. Evol. Bot.* **31**, 49–57. (doi:10.5642/aliso.20133101.08)
45. Jacobsen AL, Pratt RB, Davis SD, Ewers FW. 2007 Cavitation resistance and seasonal hydraulics differ among three arid Californian plant communities. *Plant Cell Environ.* **30**, 1599–1609. (doi:10.1111/j.1365-3040.2007.01729.x)
46. Green S, Clothier B, Jardine B. 2003 Theory and practical application of heat pulse to measure sap flow. *Agron. J.* **95**, 1371–1379. (doi:10.2134/agronj2003.1371)
47. Gorla L, Signarbieux C, Turberg P, Buttler A, Perona P. 2015 Effects of hydropeaking waves' offsets on growth performances of juvenile Salix species. *Ecol. Eng.* **77**, 297–306. (doi:10.1016/j.ecoleng.2015.01.019)
48. Ewers BE, Oren R. 2000 Analyses of assumptions and errors in the calculation of stomatal conductance from sap flux measurements. *Tree Physiol.* **20**, 579–589. (doi:10.1093/treephys/20.9.579)
49. Murray FW. 1966 On *the computation of saturation vapor pressure*. Santa Monica, CA, USA: Rand Corp.
50. Lewis S, Brando PM, Phillips OL, van der Heijden GMF, Nepstad D. 2011 The 2010 Amazon drought. *Science* **331**, 554. (doi:10.1126/science.1200807)
51. Marengo JA, Tomasella J, Alves LM, Soares WR, Rodriguez DA. 2011 The drought of 2010 in the context of historical droughts in the Amazon region. *Geophys. Res. Lett.* **38**, 1–5. (doi:10.1029/2011GL047436)

52. Salvucci ME, Osteryoung KW, Crafts-Brandner SJ, Vierling E. 2001 Exceptional sensitivity of Rubisco activase to thermal denaturation in vitro and in vivo. *Plant Physiol.* **127**, 1053–1064. (doi:10.1104/pp.010357)
53. Broedel E, Tomasella J, Cândido LA, Randow C. 2017 Deep soil water dynamics in an undisturbed primary forest in central Amazonia: differences between normal years and the 2005 drought. *Hydrol. Process.* **31**, 1749–1759. (doi:10.1002/hyp.11143)
54. Brum M *et al.* 2018 Hydrological niche segregation defines forest structure and drought tolerance strategies in a seasonal Amazon forest. *J. Ecol.* 1–16.
55. Martin-StPaul N, Delzon S, Cochard H. 2017 Plant resistance to drought depends on timely stomatal closure. *Ecol. Lett.* **20**, 1437–1447. (doi:10.1111/ele.12851)
56. Meinzer FC, Johnson DM, Lachenbruch B, McCulloh KA, Woodruff DR. 2009 Xylem hydraulic safety margins in woody plants: coordination of stomatal control of xylem tension with hydraulic capacitance. *Funct. Ecol.* **23**, 922–930. (doi:10.1111/j.1365-2435.2009.01577.x)
57. Urli M, Porté AJ, Cochard H, Guengant Y, Burlett R, Delzon S. 2013 Xylem embolism threshold for catastrophic hydraulic failure in angiosperm trees. *Tree Physiol.* **33**, 672–683. (doi:10.1093/treephys/tpt030)
58. Choat B, Brodribb TJ, Brodersen CR, Duursma RA, López R, Medlyn BE. 2018 Triggers of tree mortality under drought. *Nature* **558**, 531. (doi:10.1038/s41586-018-0240-x)
59. Adams HD *et al.* 2017 A multi-species synthesis of physiological mechanisms in drought-induced tree mortality. *Nat. Ecol. Evol.* **1**, 1285. (doi:10.1038/s41559-017-0248-x)
60. Sperry JS. 2004 Coordinating stomatal and xylem functioning–an evolutionary perspective. *New Phytol.* **162**, 568–570. (doi:10.1111/j.1469-8137.2004.01072.x)
61. Brodribb T, Holbrook N, Edwards E, Gutierrez M. 2003 Relations between stomatal closure, leaf turgor and xylem vulnerability in eight tropical dry forest trees. *Plant Cell Environ.* **26**, 443–450. (doi:10.1046/j.1365-3040.2003.00975.x)
62. Skelton RP, Brodribb TJ, McAdam SA, Mitchell PJ. 2017 Gas exchange recovery following natural drought is rapid unless limited by loss of leaf hydraulic conductance: evidence from an evergreen woodland. *New Phytol.* **215**, 1399–1412. (doi:10.1111/nph.14652)
63. Slot M, Winter K. 2017 In situ temperature response of photosynthesis of 42 tree and liana species in the canopy of two Panamanian lowland tropical forests with contrasting rainfall regimes. *New Phytol.* **214**, 1103–1117. (doi:10.1111/nph.14469)
64. Hasanuzzaman M, Nahar K, Alam MM, Roychowdhury R, Fujita M. 2013 Physiological, biochemical, and molecular mechanisms of heat stress tolerance in plants. *Int. J. Mol. Sci.* **14**, 9643–9684. (doi:10.3390/ijms14059643)
65. Suzuki N, Koussevitzky S, Mittler R, Miller G. 2012 ROS and redox signalling in the response of plants to abiotic stress. *Plant Cell Environ.* **35**, 259–270. (doi:10.1111/j.1365-3040.2011.02336.x)
66. Sperry JS, Love DM. 2015 What plant hydraulics can tell us about responses to climate-change droughts. *New Phytol.* **207**, 14–27. (doi:10.1111/nph.13354)
67. Cochard H, Coll L, Le Roux X, Ameglio T. 2002 Unraveling the effects of plant hydraulics on stomatal closure during water stress in walnut. *Plant Physiol.* **128**, 282–290. (doi:10.1104/pp.010400)
68. Cosme LH, Schietti J, Costa FR, Oliveira RS. 2017 The importance of hydraulic architecture to the distribution patterns of trees in a central Amazonian forest. *New Phytol.* **215**, 113–125. (doi:10.1111/nph.14508)
69. Sperry J. 2013 Cutting-edge research or cutting-edge artefact? An overdue control experiment complicates the xylem refilling story. *Plant Cell Environ.* **36**, 1916–1918.
70. Klein T, Yakir D, Buchmann N, Grünzweig JM. 2014 Towards an advanced assessment of the hydrological vulnerability of forests to climate change-induced drought. *New Phytol.* **201**, 712–716. (doi:10.1111/nph.12548)
71. Brodribb T, Holbrook NM. 2004 Diurnal depression of leaf hydraulic conductance in a tropical tree species. *Plant Cell Environ.* **27**, 820–827. (doi:10.1111/j.1365-3040.2004.01188.x)
72. Lin H, Chen Y, Zhang H, Fu P, Fan Z. 2017 Stronger cooling effects of transpiration and morphology of the plants from a hot dry habitat than from a hot wet habitat. *Funct. Ecol.* **31**, 2202–2211.
73. Cochard H, Delzon S. 2013 Hydraulic failure and repair are not routine in trees. *Ann. For. Sci.* **70**, 659–661. (doi:10.1007/s13595-013-0317-5)